

PAPER • OPEN ACCESS

Time-frequency analysis of acoustic waves in an integrated acousto-optical modulator based on LiNbO_3

To cite this article: A V Varlamov *et al* 2020 *J. Phys.: Conf. Ser.* **1697** 012174

View the [article online](#) for updates and enhancements.

You may also like

- [A New Direct 9-line Geometric Error Measurement Method for CNC Machine Tools](#)
Huanlao Liu, Muzammil Rasheed, Miaojing Su *et al.*
- [Environmental Characteristics of World Heritage Sites Based on High Resolution Remote Sensing Data: A Case Study of Hailongdun, Guizhou Province](#)
Youzhi An and Fujun Ma
- [AOCS General Architecture Design for SVOM Satellite](#)
Shuang Liu, Jinsong Li, Genjian Qin *et al.*



ECS
The
Electrochemical
Society
Advancing solid state &
electrochemical science & technology

DISCOVER
how sustainability
intersects with
electrochemistry & solid
state science research

Time-frequency analysis of acoustic waves in an integrated acousto-optical modulator based on LiNbO_3

A V Varlamov¹, S I Ivanov², A P Lavrov² and A V Shamray¹

¹Ioffe Institute, St. Petersburg, 194021, Russia

²Peter the Great St. Petersburg Polytechnic University, St. Petersburg, 195251, Russia

E-mail: ivanov_si@spbstu.ru

Abstract. The work presents a method allowing calculating the input admittance of an acousto-optic modulator with XY-cut lithium niobate substrate for a specific interdigital transducer structure is presented. The method does not require complex numerical computations and is sufficiently accurate. The method is based on the information about the pole of a Green's function for a given piezocrystal. A method of measuring parameters and finding the types of the excited acoustic waves based on joint time-frequency analysis using modern vector network analyzers is also presented. Good correlation between theoretical and experimental investigation is demonstrated.

1. Introduction

Acousto-optic filters and switches based on the XY-cut lithium niobate crystal are very promising since they have a low cost and can be tuned over a wide frequency range with high speed [1-4]. They are widely used in many areas of science and technology, especially in optical communication systems with wavelength division multiplexing (WDM) and in optical measuring equipment. The operation of devices discussed in this article is based on the interaction of optical and surface acoustic waves (SAW) collinearly propagating in an integrated optical structure. Waveguides for optical and acoustic waves are formed in the structure. Unfortunately, in addition to the surface acoustic wave parasitic bulk acoustic waves (including pseudo-SAW waves) are also excited in the acoustic waveguide. Bulk acoustic waves, including pseudosurface waves and surface skimming bulk waves are parasitic waves that reduce acoustic efficiency. This happens because they can propagate into the substrate thus avoiding interaction with optical waves in a LiNbO_3 waveguide. Additionally, SSBW generation may result in additional crosstalk during acoustic-optical conversion. Good suppression of crosstalk is a strict requirement for WDM communication systems' components.

The most rigorous analysis method for SAW devices is the Green's function method (GFM) [5-10]. However, its applicability is limited by its computational complexity. Therefore, the development of simplified approximate methods for calculating the properties of acoustic waves excited in an acoustic waveguide by an interdigital transducer (IDT) and methods of their direct measuring using a vector network analyzer (VNA) with a time-domain analysis option (including time gate selection).

2. Mathematical model for acoustic waves analysis

The rigorous formulation of the problem of excitation of acoustic waves in piezoelectrics by an IDT must be self-consistent meaning that the distribution of electrodes' charges is determined in the process of solving it. Such problem is solved using the Green's matrix for a linear charge, located on a selected



surface of a piezoelectric [5-10]. We introduce the coordinate system in which the crystal occupies the half-space $x_3 < 0$, and we also assume that the wave propagates in the x_1 direction, so that the wavefront of the plane wave is parallel to the x_2 axis. Mechanical displacement and fields created by a system of electrodes are written using the Green's functions of a linear charge and unknown source density $\sigma(x_1, \omega)$. Let $G_i(x_1-x'_1, \omega)$ and $G(x_1-x'_1, \omega)$ be the components of the Green's matrix of a unitary linear source, located on the surface of a crystal. Then the displacements \mathbf{u} and the potential φ of an arbitrary charge distribution $\sigma(x_1)$ in the linear approximation of the mathematical model of deformation and piezoelectric effect can be written as

$$\begin{aligned} U_i &= \int \sigma(x'_1, \omega) G_i(x_1 - x'_1, \omega) dx'_1; \\ \varphi &= \Phi(x_3=0) = \int \sigma(x'_1, \omega) G(x_1 - x'_1, \omega) dx'_1. \end{aligned} \quad (1)$$

The integration is done over the electrodes since in all other places $\sigma(x_1, \omega) = 0$. Since $G(x_1-x'_1, \omega)$ and $G_i(x_1-x'_1, \omega)$ satisfy the piezoacoustic equations and boundary conditions on the free surfaces of a piezoelectric crystal, so \mathbf{u} and φ satisfy the same conditions. At the electrodes, the condition for the jump of the normal component of the induction vector D_3 on the free surface of the piezoelectric is fulfilled $D_3(+)-D_3(-) = 4\pi\sigma(x_1, \omega)\delta(x_1-x'_1)$ – Dirac delta function. The only boundary condition that is not satisfied by equation (1) is the zero values of the tangential components of the electric field on the electrodes. Forcing this condition, we arrive to the integral equation for the charge distribution on the electrodes. This equation can be written as

$$\int \sigma(x_1, \omega) \frac{\partial G(x_3=0, x_1-x'_1, \omega)}{\partial x} dx'_1 = 0, \quad x_1 \in W. \quad (2)$$

The symbol $x_1 \in W$ means all the points on the $0x_1$ axis that belongs to electrodes.

The Cauchy principal value of the integral (2) must be calculated since the Green's function has poles of the first order. The equations (2) are the Fredholm equations of the first kind. For the XY-cut of a lithium niobate crystal the numerical solution of the equation (2) is presented in [5-10]. If the linear model of acoustic waves in a piezoelectric medium is used it is convenient to move from the (x_1, x_2, x_3, t) variables to (k_1, k_2, k_3, ω) or (\mathbf{k}, ω) variables using the Laplace transform. Vector \mathbf{k} – wave vector of an acoustic wave. The Green's function as well as other functions in the model depend on only two variables (k_1, ω) . In many works the variable is substituted by the slowness variable which is justified for a dispersionless medium where $s = \text{const}(\omega)$. In this case

$$G(k_1, \omega) = (1/\omega) \cdot G(s). \quad (3)$$

The solution of the system of equations for the mathematical model of a non-degenerate piezoelectric has eight eigenvalues, that correspond to partial waves and defines the branch points s_b of the analytic continuation of the Green's function in complex plane s . One of the poles of $G(s)$, corresponding to electrostatic interaction, is located in the origin of the coordinate system and represents the electrostatic part of the Green's function. The branch points s_{QL} , s_{QSH} and s_{QSV} of the function $G(s)$, correspond to the excitation of the quasi longitudinal (QL), quasi shear horizontal (QSH) and quasi shear longitudinal (QSL) waves. The pole at $s_0 = 0.267$ ms/m corresponds to the surface acoustic wave (SAW) excitation and the pole at $s_{psaw} = 0.228 + j0.051$ ms/m corresponds to the leaky PSAW wave. Therefore, the influence of the bulk acoustic wave QHS can be separated into SSBW and leaky PSAW waves and is given by an integral along a cut in a complex plane starting from the point $s_{QSH} = 0.225$ ms/m. The limiting value for quasi shear vertically polarized waves is $s_{QSV} = 0.2565$ ms/m and for the given LiNbO₃ cut the influence of this waves on $G(s)$ is insignificant. Asymptotic behavior of the function $G(s)$ starts at $s_{\max} \sim 0,5$ ms/m [5-10]. Let us present an approximate method of calculation of complex admittance $Y(\omega)$ with respect to frequency of an IDT with a regular grid of electrodes. If the voltage U is applied

across an IDT the current I flows through it. The ratio I/U of current and voltage phasors gives the input admittance of an IDT $Y(\omega)$. The current is mostly defined by the electrostatic charge density which contributes to the capacitive part of $Y(\omega)$. This contribution can be written explicitly by introducing the static capacitance C_e :

$$Y(\omega) = G_a(\omega) + jB_a(\omega) + j\omega C_e = Y_a(\omega) + j\omega C_e. \quad (4)$$

In this equation $G_a(\omega)$ and $B_a(\omega)$ represent the real and imaginary parts of $Y_a(\omega)$, contributed by the surface charge density $\sigma_a(x, \omega)$. Using the results from [11] for the electrostatic charge density calculation the following first order approximation of the admittance $Y_a(\omega)$

$$Y_a(\omega) = \omega W / 2\pi j \int_{-\infty}^{\infty} \left[\frac{\sin(Nkp)}{\sin(kp)} \right]^2 \rho_f^2(k) G_s(k, \omega) dk, \quad (5)$$

where N – the total number of IDT electrodes; W – electrode length; p – electrode grid period; a/p – metallization coefficient; $\rho_f^2(k)$ – base charge density given in [11].

The Green's function $G_s(\omega)$ in equation (5) produced by the acoustic surface charge density $\sigma_a(x, \omega)$, is given by

$$G_s(k, \omega) = G_s(\omega s, \omega) = G'_s(\omega s) \otimes \{\pi\delta(\omega s) - j/(\omega s)\}, \quad (6)$$

Where operator \otimes means convolution of $G'_s(\omega s)$ and $\{\pi\delta(\omega s) - j/(\omega s)\}$; the Green's function $G'_s(\omega s)$ is equal to the Green's function $G(s)$ given by equation (3), except for the first term responsible for quasistatic interaction.

From equation (6) it follows the imaginary $B_a(\omega)$ and real $G_a(\omega)$ parts of the admittance $Y(\omega)$ are related to each other by the Hilbert transform [11], which also follows from the cause and effect relation between the current and voltage.

The equations (4) – (6) allow calculation of the input admittance $Y(\omega)$ of an IDT caused by the excitation of the acoustic wave in a piezoelectric for a given Green's function and IDT parameters and compare theoretical and experimental results.

3. Measurement results and discussion

An integrated modulator on a lithium niobate substrate was experimentally investigated [12]. The modulator configuration is shown in figure 1 and it is based on a XY-cut monocrystalline plate. In fact, the modulator test structure with 3 IDT is shown in the figure.

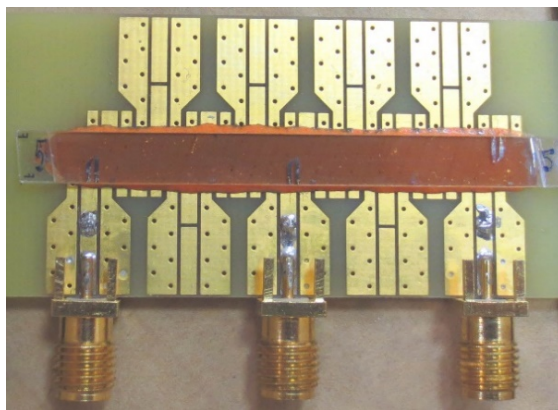


Figure 1. Outline of the integrated modulator with three IDT.

The walls of the acoustic waveguide are formed by thermal diffusion of titanium along the Y direction, the distance between the walls is $100\ \mu\text{m}$. Aluminum IDT with $N = 17$ fingers and $200\ \text{nm}$ thickness are formed on the surface of the acoustic waveguide by magnetron deposition. The IDT period (the electrodes step) is $p = 10\ \mu\text{m}$, $a/p = 0.5$, the distance between two adjacent IDTs is $l = 21\ \text{mm}$, the overlap of the electrodes is $W = 100\ \mu\text{m}$, and the substrate thickness is $1\ \text{mm}$. The ends of the acoustic waveguide are terminated by absorbers. The compensation angle between the normal to the electrodes and the crystallographic Y axis is approx. 5° [12].

Microwave devices and circuits are most effectively investigated using vector network analyzers (VNA). Modern VNAs often have a software option allowing to do time domain measurements including application of time windows for different (separate) signal components selection [13]. This type of analysis has significant advantages in many practical applications including measuring parameters of microwave SAW devices.

Microwave devices and circuits are most effectively investigated using vector network analyzers (VNA). Modern VNAs often have a software option allowing to do time domain measurements including application of time windows for different (separate) signal components selection [13]. This type of analysis has significant advantages in many practical applications including measuring parameters of microwave SAW devices.

Figure 2 shows the amplitude and phase of the reflection coefficient at the input of a split-electrode modulator over a wide frequency band. The transducer has two resonances, one at approx. $190\ \text{MHz}$ and another at approx. $550\ \text{MHz}$, corresponding to the first and third harmonics of the transducer. The low frequency resonance corresponds to the SAW excitation while the high frequency resonance corresponds to the parasitic quasi shear horizontally polarized bulk wave. The reflection coefficient behavior around $320\ \text{MHz}$ is defined by the influence of parasitic bulk wave with quasi longitudinal polarization. The contribution of the bulk QL wave in the modulator response is limited by SSBW wave, and the contribution of QSH wave includes SSBW and PSAW waves.

Figure 3 shows the graphs of the real and imaginary parts of the admittance $Y(\omega)$ of the modulator measured by a VNA. The values of s_{QL} , s_{QSH} , and s_0 , calculated using these graphs are in good agreement with theoretical calculations by the method described in Section 2. The measurement results presented in figure 3 show that the real and imaginary parts of the admittance $Y(\omega)$ are related to each other by the Hilbert transform.

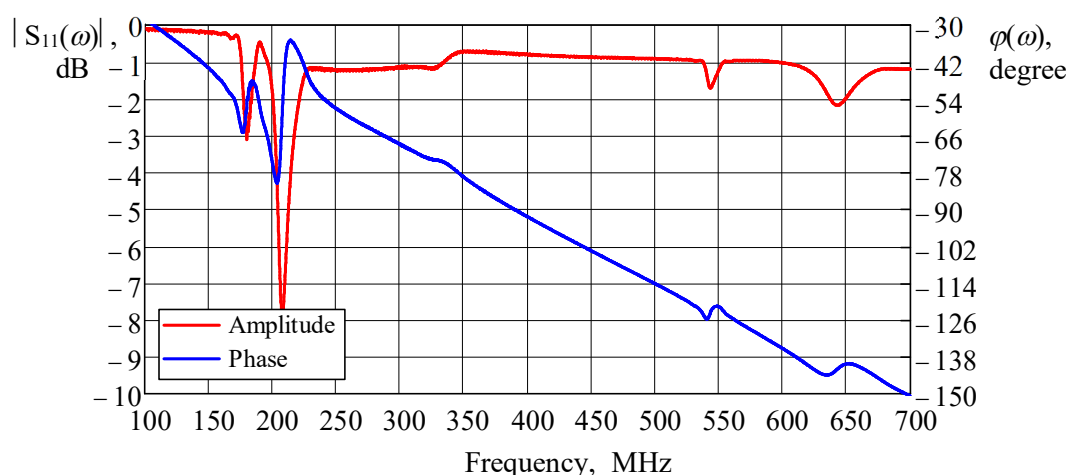


Figure 2. Amplitude and phase of the input reflection coefficient of a 17 finger IDT with split-electrode configuration.

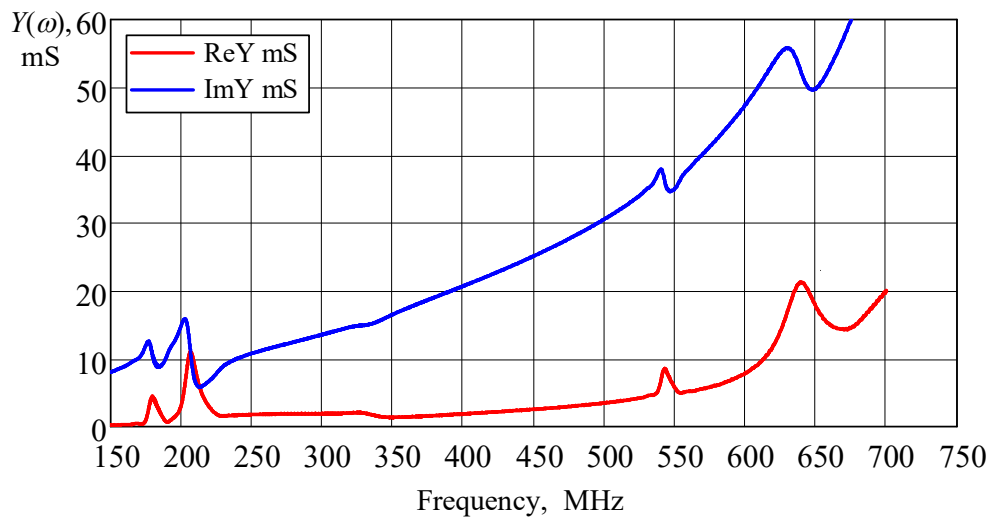


Figure 3. The real and imaginary parts of the input admittance $Y(\omega)$ of the modulator.

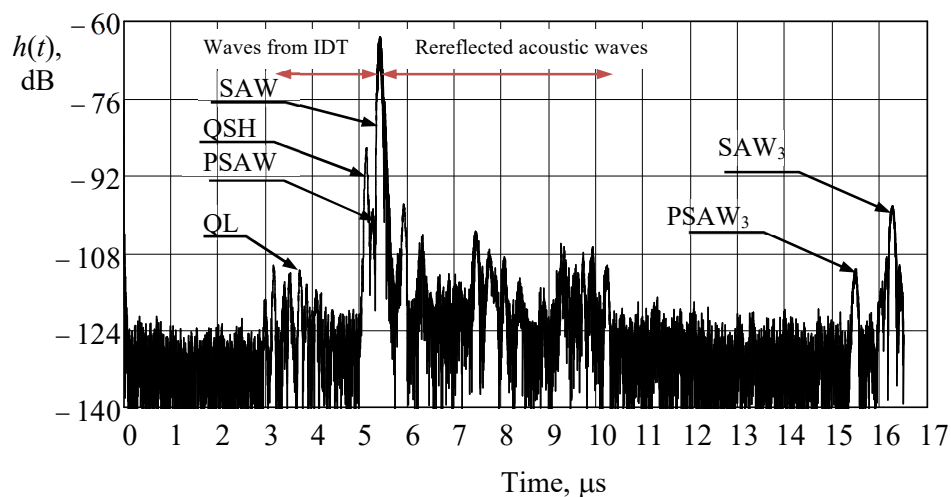


Figure 4. The output response of an acousto-optic modulator to an input δ -pulse.

Additional information about the acoustic waves excited in the substrate can be obtained by analyzing together the characteristic of the output response $h_{21}(t)$ of the acousto-optic modulator to the input $\delta(t)$ -pulse and the frequency response $|S_{21}(\omega)|$, obtained after selection (based on $h_{21}(t)$ structure), of the time gates, these gates correspond to the intervals where the type of the excited wave can be anticipated. A time-gate selection and for this specific time interval the response $|S_{21}(\omega)|$ calculation – it is software option in some VNAs. In figure 4 one can see the results of such analysis, the time localization of various types of acoustic waves exciting the second (see figure 1) IDT in the acousto-optic modulator is noted. The second IDT is used as the SAW probe (receiver).

4. Conclusion

The rigorous mathematical model that describes the results of excitation of acoustic waves in devices with a piezoelectric substrate requires significant computational resources and as a result has only limited application in the engineering practice. On the other hand, the Green's functions for various cuts

of piezoelectric crystals (including lithium niobate) are sufficiently available. In this work the method of calculation of the input impedance of the acousto-optic modulator on the XY-cut LiNbO₃ substrate for a specific IDT structure is presented. The method does not require complex numerical computations and is sufficiently accurate. In addition, a method of measuring parameters and finding the types of the excited acoustic waves based on joint time-frequency processing using modern vector network analyzers is presented. Good correlation between the theoretical and experimental results is demonstrated in research.

Acknowledgments

The reported study was funded by RFBR, project number 20-07-00928\20.

References

- [1] Nakazawa T, Taniguchi S and Seino M 1999 Ti:LiNbO₃ acoustooptic tunable filter (AOTF) *Sci. Tech. J.* **35** 107–12
- [2] Herrman H and Mendis H 1999 Broadly tunable integrated acoustooptical polarization converters in LiNbO₃ *Proc. 9th Europ. Conf. on Integrated Optics (Torino, Italy)* pp 229–32
- [3] Manzanegue T, Lu R, Yang Y and Gong S 2019 Low-loss and wideband acoustic delay lines *IEEE Trans. on Microwave Theory and Techn.* **67** 1379-91
- [4] Pang X and Yong Y-K 2019 Simulation of nonlinear resonance, amplitude-frequency, and harmonic generation effects in SAW and BAW devices *IEEE Trans. on Ultrasonics, Ferroelectrics, and Frequency Control* **67** 422-30
- [5] Peverini O A, Orta R and Tascone R 2000 Full-wave modeling of piezoelectric transducers for SAW acousto-optical interactions *Optical and Quantum Electronics* **32** pp 855-67
- [6] Baghai-Wadji A R, Manner O and Ganr-Puchstein R 1989 Analysis and measurement of transducer end radiation in SAW filters on strongly coupling substrates *IEEE Trans. on Microwave Theory and Techn.* **37** 150-8
- [7] Peverini O A, Orta R and Tascone R 2001 A new reduced-order model of SAW interdigital transducers *IEEE Trans. on Microwave Theory and Techn.* **49** 1785-91
- [8] Peverini O A, Orta R and Tascone R 2002 A fast Green's function method for the analysis of IDT's for acousto-optical devices *IEEE Trans. on Ultrasonics, Ferroelectrics, and Frequency Control* **49** 365-73
- [9] Peverini O A, Orta R and Tascone R 2002 Analysis of piezoelectric strip waveguides based on the effective index and pseudospectral element methods *J. Acoust. Soc. Am.* **112** 2623-33
- [10] Milsom R F, Reilly N H C and Redwood M 1977 Analysis of generation and detection of surface and bulk acoustic waves by interdigital transducers *IEEE Trans. on Sonics and Ultrasonics* **24** 147-66
- [11] Morgan D P 1985 *Surface-Wave Devices for Signal Processing* (Amsterdam: Elsevier)
- [12] Varlamov A V and Shamray A V 2019 Optimal configuration of the waveguide acousto-optic TE-TM polarization mode convertor on X-cut lithium niobate substrate *J. Phys.: Conf. Series* **1236** 012034
- [13] Dunsmore P 2014 *Handbook of Microwave Component Measurements: with Advanced VNA Techniques* (New York: John Wiley & Sons, Ltd.) chapter 4 pp 266–302